土木与环境工程学报(中英文)
Journal of Civil and Environmental Engineering
ISSN 2096-6717,CN 50-1218/TU

《土木与环境工程学报(中英文)》网络首发论文

题目：基于基因表达编程和粒子群优化鲁棒混合计算模型的深部地下矿井岩爆分类（英文）
作者：Quang-Hieu TRAN，Xuan-Nam BUI，Hoang NGUYEN
收稿日期：2021-11-16
网络首发日期：2022-03-19
引用格式：Quang-Hieu TRAN，Xuan-Nam BUI，Hoang NGUYEN．基于基因表达编程和粒子群优化鲁棒混合计算模型的深部地下矿井岩爆分类（英文）[J/OL]．土木与环境工程学报(中英文).
https://kns.cnki.net/kcms/detail/50.1218.TU.20220317.1347.002.html

Published online：2022-03-19 17:52:59
URL：https://kns.cnki.net/kcms/detail/50.1218.TU.20220317.1347.002.html

DOI: 10.11835/j.issn.2096-6717.2022.023　　开放科学（资源服务）标识码（OSID）：

Classifying rockburst in deep underground mines using a robust hybrid computational model based on gene expression programming and particle swarm optimization

Quang-Hieu TRAN, Xuan-Nam BUI, Hoang NGUYEN
(Department of Surface Mining, Mining Faculty; Innovations for Sustainable and Responsible Mining (ISRM) Research Group, Hanoi University of Mining and Geology, Hanoi 100000, Vietnam)

Abstract: In deep underground mining, rockburst is taken into account as an uncertainty risk with many adverse effects (i.e., human, equipment, tunnel/underground mine face, and extraction periods). Due to its uncertainty characteristics, accurate prediction and classification of rockburst tendency are challenging, and previous results are poor. Therefore, this study proposed a robust hybrid computational model based on gene expression programming (GEP) and particle swarm optimization (PSO), called GEP-PSO, to predict and classify rockburst tendency in deep openings with an accuracy improved. A different number of genes (from 1 to 4) and linking functions (e.g., addition, extraction, multiplication, and division) in the GEP model were also evaluated during the development of the GEP-PSO model aim. Geotechnical and constructive factors of 246 rockburst events were collected and used to develop the GEP-PSO models in terms of rockburst classification. Subsequently, a robust technique to handle missing values of the dataset was applied to improve the dataset's attributes. The last step in the data processing stage is the feature selection to select potential input parameters using a correlation matrix. Finally, 13 hybrid GEP-PSO models were developed with different accuracies reported. The findings indicated that the GEP-PSO model with three genes in the structure of GEP and the multiplication linking function provided the highest accuracy (i.e., 80.49%). The obtained results of the best GEP-PSO model were then compared with a variety of previous models developed by previous researchers based on the same dataset. The comparison results also showed that the selected GEP-PSO model results outperform those of previous models. In other words, the accuracy of the proposed GEP-PSO model was improved significantly in terms of prediction and classification of rockburst grade. It can be considered widely applied in deep openings aiming to predict and evaluate the rockburst susceptibility accurately.
Keywords: rockburst; GEP-PSO model; underground-mining; deep openings; risk assessment

基于基因表达编程和粒子群优化鲁棒混合计算模型的深部地下矿井岩爆分类

Quang-Hieu TRAN, Xuan-Nam BUI, Hoang NGUYEN
(Department of Surface Mining, Mining Faculty; Innovations for Sustainable and Responsible Mining (ISRM) Research Group, Hanoi University of Mining and Geology, Hanoi 100000, Vietnam)

摘　要：在深部地下采矿中，岩爆因具有许多不利影响（如，对人员、设备、隧道/地下矿山工作面和开采周期等的影响）而被视为不确定性风险。由于其不确定性的特征，对岩爆趋势的准确预测和分类具有一定难度，且已有研究成果较少。提出一种基于基因表达编程（GEP）和粒子群优化（PSO）的鲁棒混合计算模型 GEP-PSO，用于预测和分类深部开口的岩爆趋势，提高了预测和分类的准确性。在建立 GEP-PSO 模型过程中，评估了 GEP 模型中不同数量的基因（1~4）和连接功能（例如，加法、提取、乘法和除法）。收集了 246 次岩爆发生的地质和施工因素，用于建立岩爆分类的 GEP-PSO 模型；应用处理数据集缺失值的技术改进数据集的属性；用相关矩阵选取潜在输入参数的特征；建立了 13 个混合 GEP-PSO 模型，得到了各模型的精度。结果表明：在 GEP 结构中具有 3 个基因和乘法连接函数的 GEP-PSO 模型具有最高的准确度（80.49%）。将获得的最佳 GEP-PSO 模型的结果与基于相同数据集开发的各种已有模型进行比较，结果表明：选择的 GEP-PSO 模型结果优于已有模型，表明提出的 GEP-PSO 模型在岩爆等

Received: 2021-11-16
Author brief: Quang-Hieu TRAN (corresponding author): PhD, main research interest: rock mechanics; blasting, occupational safety and health in mining, E-mail: tranquanghieu@humg.edu.vn.

级的预测和分类方面的准确性显著提高，可以应用于深开挖工程中，以准确预测和评估岩爆敏感性。

关键词：岩爆；GEP-PSO 模型；地下采矿；深开挖；风险评估
中图分类号：TU457；TD311　　**文献标志码**：A

1 Introduction

In the mining industry, especially in underground mines and tunnels, a sudden, violent rupture or highly stressed rock collapse is considered natural hazards with extreme risks [1-2], and it is called rockburst. Some rockburst events occurred, and their destruction level are presented in Fig. 1. This phenomenon is becoming increasingly common in recent years, especially in complex mining conditions and deep openings [7-8]. The rockburst problem has claimed the lives of hundreds of miners and many other valuable assets in United States, Germany, Australia, China, Canada, and other countries [9-14].

Understanding the risks and inherently dangers of rockburst, many scholars efforted to assess the risk of rockburst based on various approaches, such as seismic computed tomography detection [15], static and dynamic stresses [16], distance [2], geomechanics [8,17], to name a few. The evaluations showed that the rockburst susceptibility and the influential parameters are a critical overview of this phenomenon to forecast or prevent this happen. Nevertheless, along with these evaluations, the rockburst phenomenon has not been predicted, which is challenging for researchers.

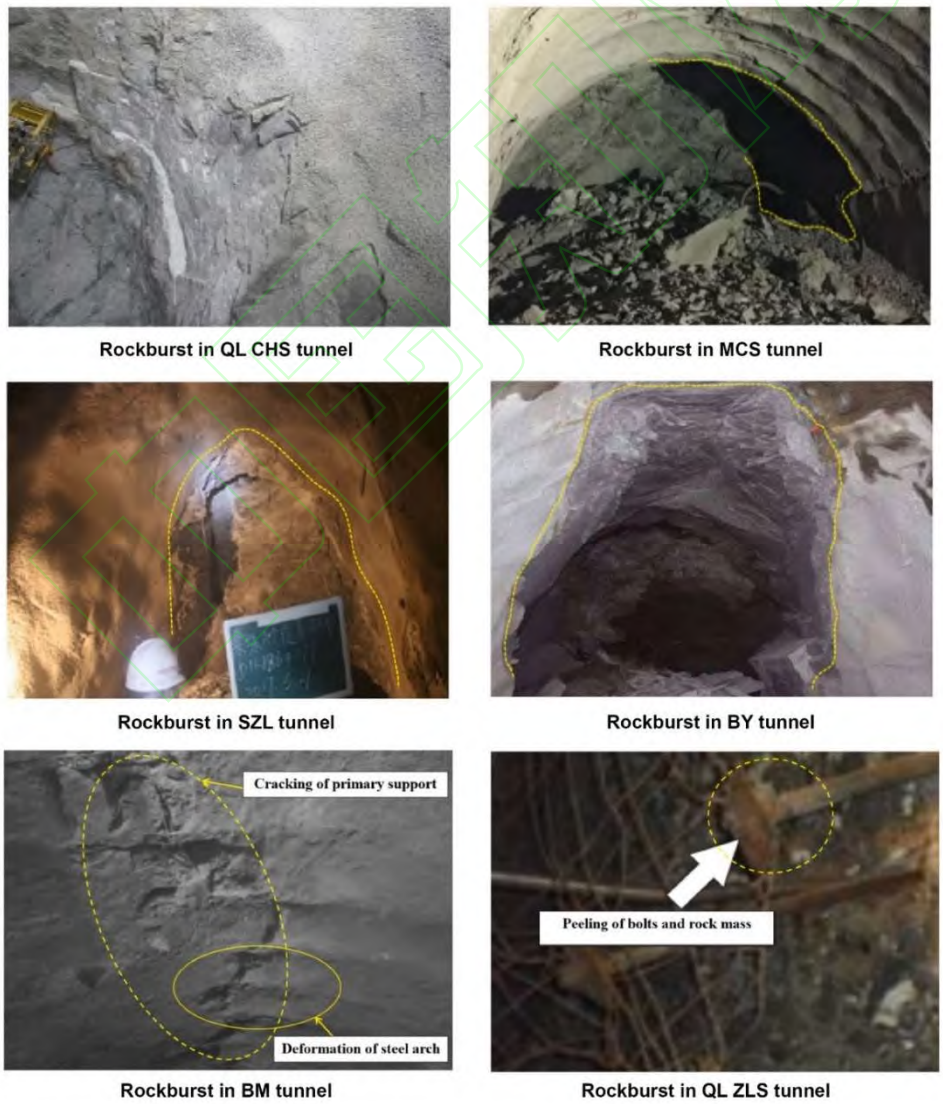

Fig. 1 Some rockburst events occurred and their destruction level [3-6]

Based on previous researchers' evaluations, several scientists applied state-of-the-art computational models to forecast the rockburst susceptibility in deep openings. It is worth mentioning that soft computing models were not only applied in rockburst forecasting but also in geotechnical and geoengineering [18-26]. For instance, Dong et al. [27] used the Random Forest (RF) algorithm to predict the possible rockburst tendency. In another study, Wang et al. [28] applied the fuzzy matter-element model to predict the rockburst tendency, and it was confirmed as a reliable model to solve this problem. Based on the mechanism of rockburst and mining conditions (e.g., position, depth, rockburst magnitude, initiation time, distribution), Cai [29] used empirical computational models with in situ stress measurement, 3D numerical modeling analysis, and laboratory tests to predict and prevent the rockburst grade. Besides, Zhou et al. [30] developed various supervised learning models for predicting rockburst tendency, including k-nearest neighbor (KNN), multilayer perceptron neural network (MLPNN), random forest (RF), linear discriminant analysis (LDA), Naïve Bayes (NB), gradient-boosting machine (GBM), quadratic discriminant analysis (QDA), partial least-squares discriminant analysis (PLSDA), support vector machine (SVM), and classification tree (CT). Finally, they found that the GBM is the best model for classifying the rockburst tendency. A decision tree model was also applied by Pu et al. [31] to predict the rockburst potential. Different accuracies with acceptable results were reported in their study. By another approach, Pu et al. [32] applied the SVM model with the support of the t-distributed stochastic neighbor embedding and clustering technique for predicting rockburst. Eventually, they concluded that the proposed model based on the SVM model is a potential model with wide applications in the rockburst prediction. Zhou et al. [33] also converted this classification problem to a regression problem and applied a hybrid model based on artificial neural network (ANN) and artificial bee colony (ABC) to predict rockburst, and it is considered as another approach to predict rockburst. Based on the particle swarm optimization (PSO), Xue et al. [34] also developed an extreme learning machine (ELM) model to predict rockburst with a promising result. Faradonbeh et al. [35] also applied the fuzzy C-means (FCM) and self-organizing map (SOM) techniques to predict rockburst tendency. An accuracy of 75.8% was reported in their study for the FCM model, and is up to 100% for the SOM model. Nevertheless, only 58 rockburst events were used in this study, and it is a small database that can not be represent for other areas. Zhang et al. [36] also applied a variety of ensemble machine learning models, such as ANN, SVM, KNN, NB, and logistic regression for predicting rockburst intensity using 188 rockburst intances. They indicated that the ensemble model can classify rockburst better than single models witn an improvement of 15.4%. He et al. [37] also evaluated and predicted the rockburst behaviors in 13 deep traffic tunnels in China. Nonetheless, only empirical equations were applied in their study. In another study, Zhou et al. [38] developed the firefly algorithm-based ANN model (FA-ANN) for classifying rockburst with a potential solution that can support underground mines and tunnels determine and prevent hazardous under different conditions.

Although many soft computational models have been proposed to predict the rockburst tendency; however, their accuracy is still limited, and the accuracy of computational models is a challenge. Therefore, this study presented a novel method to improve computational models' accuracy for classifying rockburst susceptibility, namely GEP-PSO. Indeed, the gene express programming (GEP) will be applied to classify the rockburst grade; meanwhile, the PSO algorithm plays a role as an optimization tool to improve the GEP model's accuracy. Furthermore, a different number of genes and linking functions will be surveyed to discover their feasibility and accuracy in terms of rockburst classification and evaluation. The details of this methodology and obtained results are presented in the next sections.

2 Principle of the machine learning algorithms used

As stated above, this study aims to classify and evaluate the rockburst phenomenon's capacity in deep openings by a novel combination of the PSO algorithm and GEP. Therefore, this section focuses on the PSO and GEP models' principles to propose the PSO-GEP model framework.

2.1 Gene expression programming (GEP)

GEP is well-known as an evolutionary theory proposed by Ferreira [39] based on genetic programming (GP) and parse trees. Therefore, it uses similar GP parameters, such as terminal conditions, function set, control parameters, terminal set, and fitness function [40]. GEP has greatly surpassed and extremely versatile the existing evolutionary techniques since it inherited the advantages from GP, i.e., the expressive parse trees of varied shapes and sizes [41]. In brief, the evolution process of GEP can be explained through the following steps:

Step 1: Initialization

In this step, the initial chromosomes are set equal to the population dimension, and they are generated randomly. Herein, each chromosome consists of genes, and they are organized based on

structures (head and tail) aiming to create a valid solution [41]. This stage is also called Karva, and it can represent any mathematical or logical expression with different sizes and shapes. Accordingly, all chromosomes are converted to expression trees, and then the generated solutions are performed to obtain the fitness values.

Step 2: Selection and reproduction

In this step, the operator would select programs to replicate the operator to copy into a new generation a chromosome with high fitness. The potential individuals are specified for the next generation based on their fitness through the roulette wheel selection. They are considered the main factors to guarantee the cloning and survival of the new population's best chromosomes. In the new population, the genetic operations are applied to manipulate during reproduction process based on randomly selected chromosomes genetically. Thus, a chromosome in GEP might be modified to better fit individuals in the new generation. The genetic operations are applied during the reproduction process, including mutation, insertion sequence transposition, root insertion sequence transposition, gene transposition, single and double crossover, gene crossover, and inversion.

Step 3: Termination

The program executes the steps above and repeats for a certain number of generations or satisfied the stopping conditions (i.e., lowest error for population). Finally, the best expression tree is found out and exported as the output of the problem. The flowchart of GEP is shown in Fig. 2, and its pseudo-code is presented in Fig. 3.

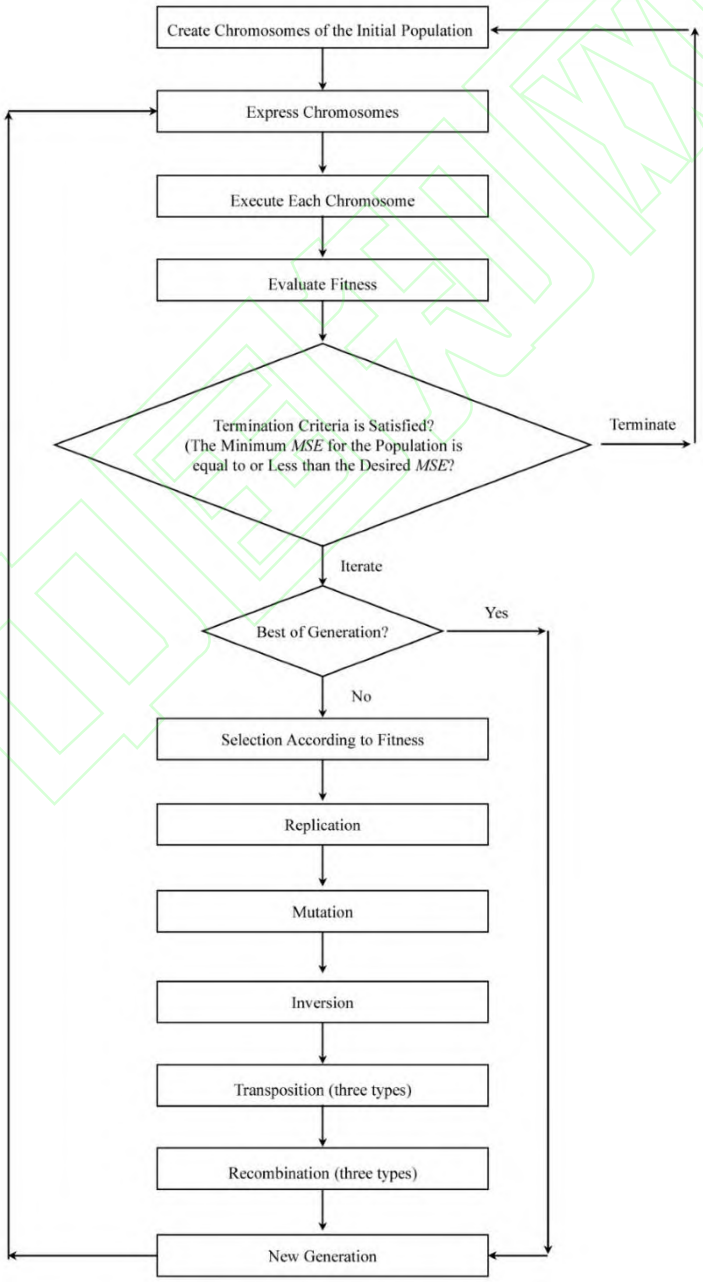

Fig. 2 The procedure of the GEP algorithm

GEP algorithm

Input: Generation $_{max}$, Population $_{size}$, Genes $_{numbers}$, Head $_{length}$, Function $_{set}$, Terminal $_{set}$, Constants $_{per\ gene}$, DC $_{limit}$
Crossover $_{rate}$, Mutation $_{rate}$, Inversion $_{rate}$, Transposition $_{rate}$
Output: Solution $_{Best\text{-}Cost}$, Solution $_{Best\text{-}ET}$
// **Initialization**//
1. population ⟵ initialize population (Population $_{size}$, Genes $_{numbers}$, Head $_{length}$, Function $_{set}$, Terminal $_{set}$, Constants $_{per\ gene}$, DC $_{limit}$)
2. **for** each Solution $_i$ ∈ population **do**
   // Translate the Chromosome into Expression Tree //
3. Solution $_{i\_ET}$ ⟵ translate breadth first (Solution $_{i\_genes}$)
   // Execute the Corresponding Expression Tree//
4. Solution $_{i\_cost}$ ⟵ execute (Solution $_{i\_ET}$)
5. **end**
   // **Elitist selection & Replication** //
6. Solution $_{Best}$ ⟵ select best solution (population)
7. population ⟵ copy Solution $_{Best}$
8. **while** stopping condition are not met **do**
   // **Parent Selection Process**//
9. parent $_i$ ⟵ select parents (population)
10. parent $_j$ ⟵ select parents (population)
   // **Crossover operator**//
11. offspring $_1$ ⟵ crossover (parent $_i$, parent $_j$, Crossover $_{rate}$)
12. offspring $_2$ ⟵ crossover (parent $_j$, parent $_j$, Crossover $_{rate}$)
   // **Mutation operator** //
13. offspring $_{1m}$ ⟵ mutation (offspring $_1$, Mutation $_{rate}$)
14. offspring $_{2m}$ ⟵ mutation (offspring $_2$, Mutation $_{rate}$)
   // **Inversion operator** //
15. offspring $_{1\_inversion}$ ⟵ inversion (offspring $_{1m}$, Inversion $_{rate}$)
16. offspring $_{2\_inversion}$ ⟵ inversion (offspring $_{2m}$, Inversion $_{rate}$)
   // **Transposition operator** //
17. offspring $_{1\_transposition}$ ⟵ inversion (offspring $_{1\_inversion}$, Transposition $_{rate}$)
18. offspring $_{2\_transposition}$ ⟵ inversion (offspring $_{1\_inversion}$, Transposition $_{rate}$)
   // **Traslate the Choromosme into Experession Tree**//
19. offspring $_{1\_ET}$ ⟵ translate breadth first (offspring $_{1\_transposition}$)
20. offspring $_{2\_ET}$ ⟵ translate breadth first (offspring $_{2\_transposition}$)
   // **Execute the Corresponding Expression Tree** //
21. offspring $_{1\_cost}$ ⟵ execute (offspring $_{1\_ET}$)
22. offspring $_{2\_cost}$ ⟵ execute (offspring $_{2\_ET}$)
   // **Roulette Wheel Selection** //
23. population ⟵ population update RWS (offspring $_{1\_cost}$, offspring $_{2\_cost}$)
24. **end**
25. return to best soloution

Fig. 3 Pseudo-code of the GEP algorithm

2.2 Particle swarm optimization (PSO)

PSO is well-known as a robust metaheuristic algorithm that was successfully applied for different optimization problems [42-46]. It was proposed by Kennedy and Eberhart [47] based on the nature-based behaviors of swarms (e.g., flock birds, bee, ant). These behaviors are simulated under the moving around the search space of the particles in the swarm. Each individual is assigned a position (x_i), and they fly around the search space with a velocity (v_i). For each position, each particle's fitness is evaluated and recorded, and the best fitness (P_{best}) is shared with the other individuals. Each particle keeps track of the best fitness and expands the search space to find out the better position (G_{best}). The searching process might be repeated many times to obtain satisfying values. The optimization process of the PSO algorithm is illustrated in Fig. 4. Further details of the PSO algorithm can be read in the literature [48-54].

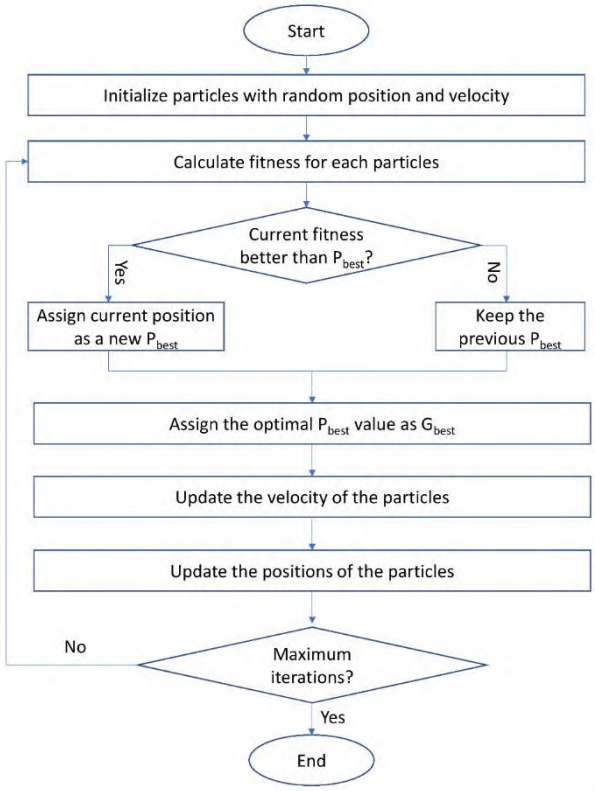

Fig. 4 Optimization procedure of the PSO algorithm

2.3 PSO-based GEP model for classifying rockburst in deep openings

As the primary purpose of this study, the GEP-PSO framework is considered and proposed in this section, aiming to improve the classification model of rockburst, i.e., GEP. Accordingly, a mathematical equation would be offered based on a customized combination of PSO and GEP using the dependent variables. In the first step, GEP is applied to build a mathematical with an acceptable ROC curve result. Subsequently, the established chromosomes are used as the main parts of the modified GEP models in the next step. The chromosomes are then embedded in the PSO algorithm to determine a better performance of the ROC curve based on the correct structure of the GEP model, called the GEP-PSO model. Note that the number of genes and linking functions are taken into account as the vital parameters of the GEP models, and the performance of the GEP models is highly dependent on these parameters.

Furthermore, in each GEP model, weights (or coefficients) are often determined based on the dataset's characteristics and the chromosomes, genes, and linking function. However, weights can be adjusted to get better accuracy for the GEP models based on a specific number of genes and linking functions.

In order to embed the PSO algorithm to GEP models, an initial number of populations is necessary for the optimization process of the PSO algorithm, and they might repeat many times to obtain a better ROC curve value. The PSO algorithm can modify the GEP model's coefficients to get higher ROC curve values. The algorithm would stop when the best ROC value is reached (satisfied), or the searching is repeated with the specified iterations. The framework is proposed in Fig. 5.

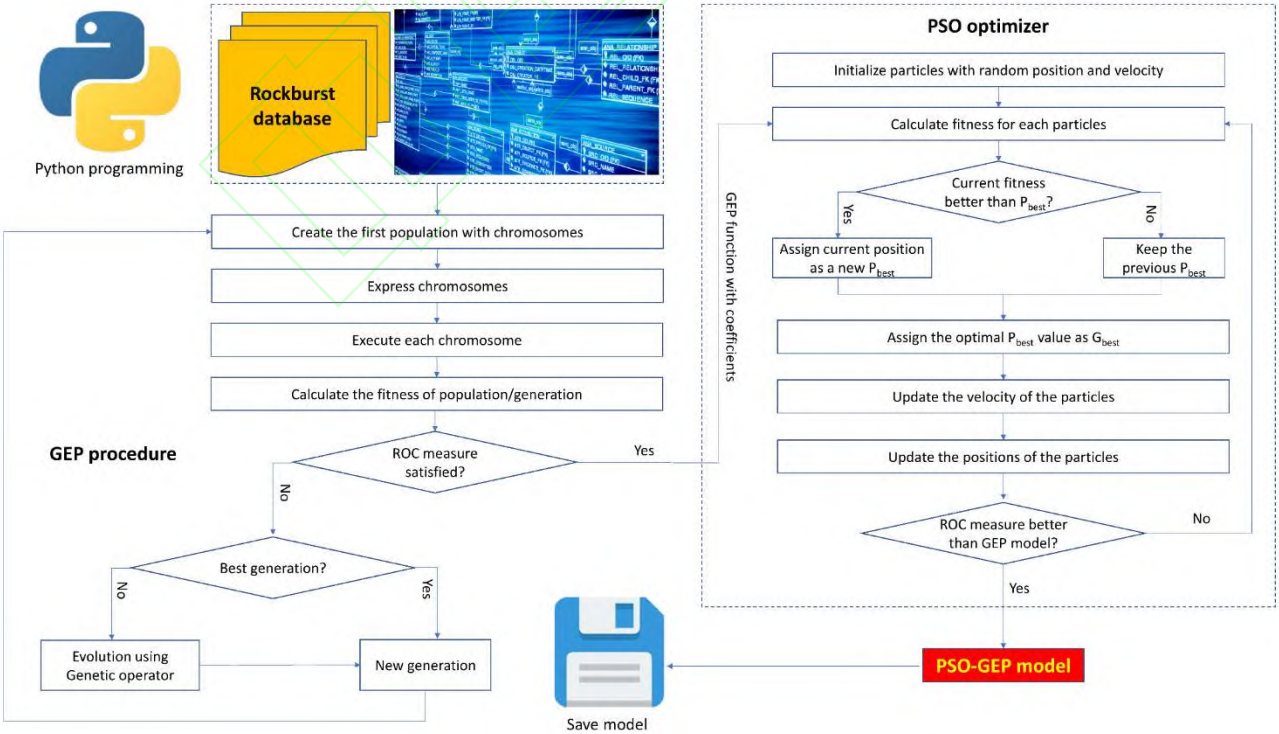

Fig. 5 Proposed hybrid PSO-GEP algorithm for classifying rockburst

3 Data acquisition and processing

3.1 Data acquisition

First of all, it is necessary to emphasize that rockburst is a dangerous phenomenon in deep underground mines and tunnels, as mentioned above. It is difficult to observe these phenomena, and it is challenging to collect a dataset with multiple observations. Therefore, many previous researchers efforted to collect and merge many cases from different deep underground mines and tunnels [27, 55-56] as a dataset. Finally, 246 rockburst samples were collected in previous studies (Fig. 6), and they were summarized by Zhou et al. [30] and used to investigate and evaluate the performance of the proposed model in this study.

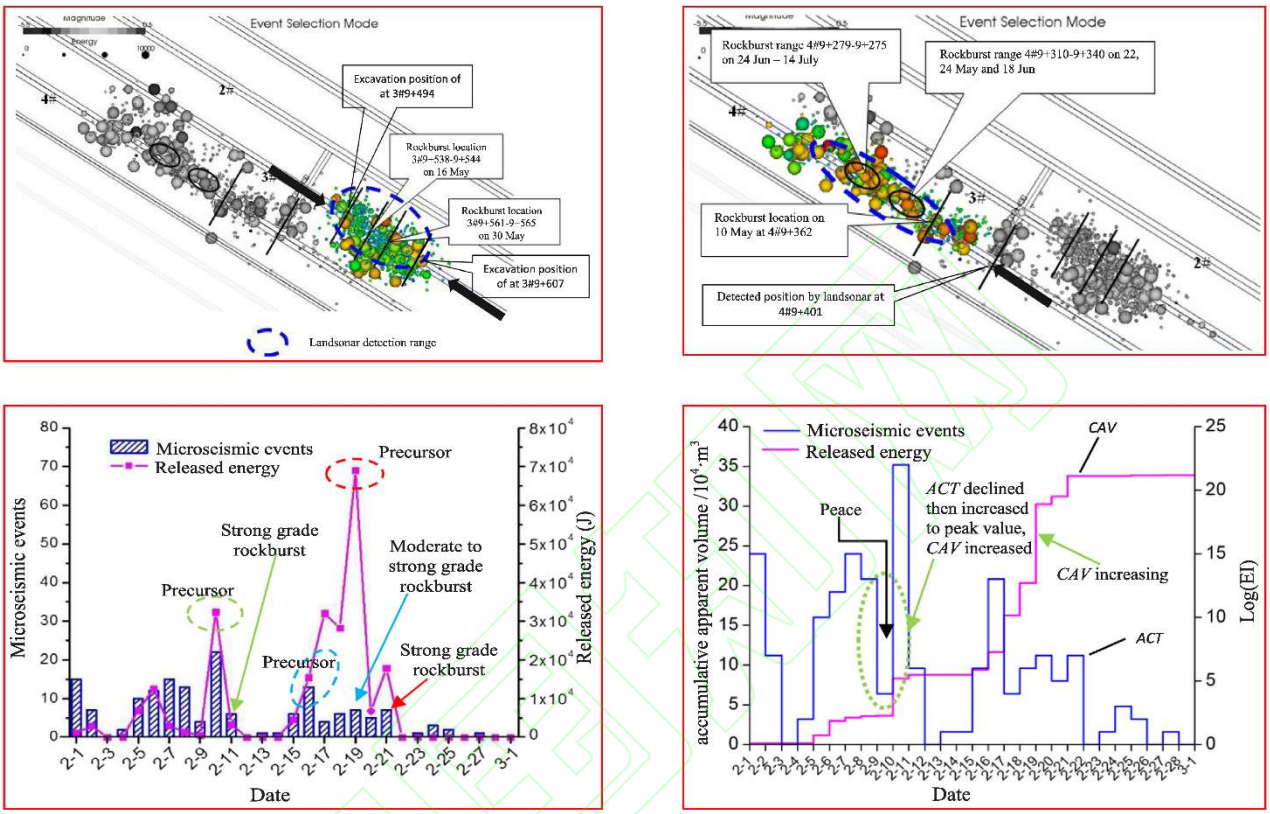

Fig. 6 Data collection of the rockburst events using microseismic systems and some results (Modified after Ma et al. [57])

From the various datasets collected, there are 12 variables recorded, including the depth of underground caverns (X_1), maximum tangential stress of the cavern wall (X_2), uniaxial compressive strength (X_3), uniaxial tensile strength (X_4), stress concentration factor (X_5), X_6-X_{10} are indexes of rock mass related to X_3 and X_4 and they are calculated as described in equations (1)-(5), elastic strain index (X_{11}), and the rockburst ability (Y).

$$X_6 = \frac{X_3}{X_4} \quad (1)$$

$$X_7 = \frac{X_3 - X_4}{X_3 + X_4} \quad (2)$$

$$X_8 = \frac{X_3 \times X_4}{2} \quad (3)$$

$$X_9 = \frac{\sqrt{X_3 \times X_4}}{2} \quad (4)$$

$$X_{10} = \sqrt{\frac{X_3 \times X_4}{2}} \quad (5)$$

3.2 Processing the collected rockburst dataset

Before developing the classification models for rockburst, the collected dataset should be processed and prepared to ensure the dataset's generalized characteristics and avoid overfitting the models. An analysis shows that some values in the first variable are missed, and they are variance account for 13% of the whole number of observations, as illustrated in Fig. 7.

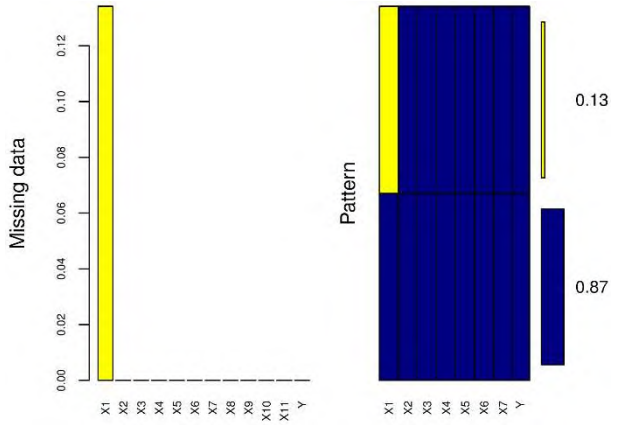

Fig. 7 Processing the missing data of rockburst

In this case, there are three options for solving the X_1 variable, including removing the entire of this variable, removing rows with missing values, or filling the missing values. However, given the effects of the input variables, many researchers indicated that X_1 significantly impacts the probability of rockburst in deep openings. Therefore, the X_1 variable was kept on. Also, to avoid reducing the dataset's size, the rows with missing values were kept on as well. Finally, a data processing technique has been applied to fill the missing values to the collected dataset, namely "mean column values" [58]. The processed dataset's input variables were then visualized as a scatter plot to show their characteristics (Fig. 8).

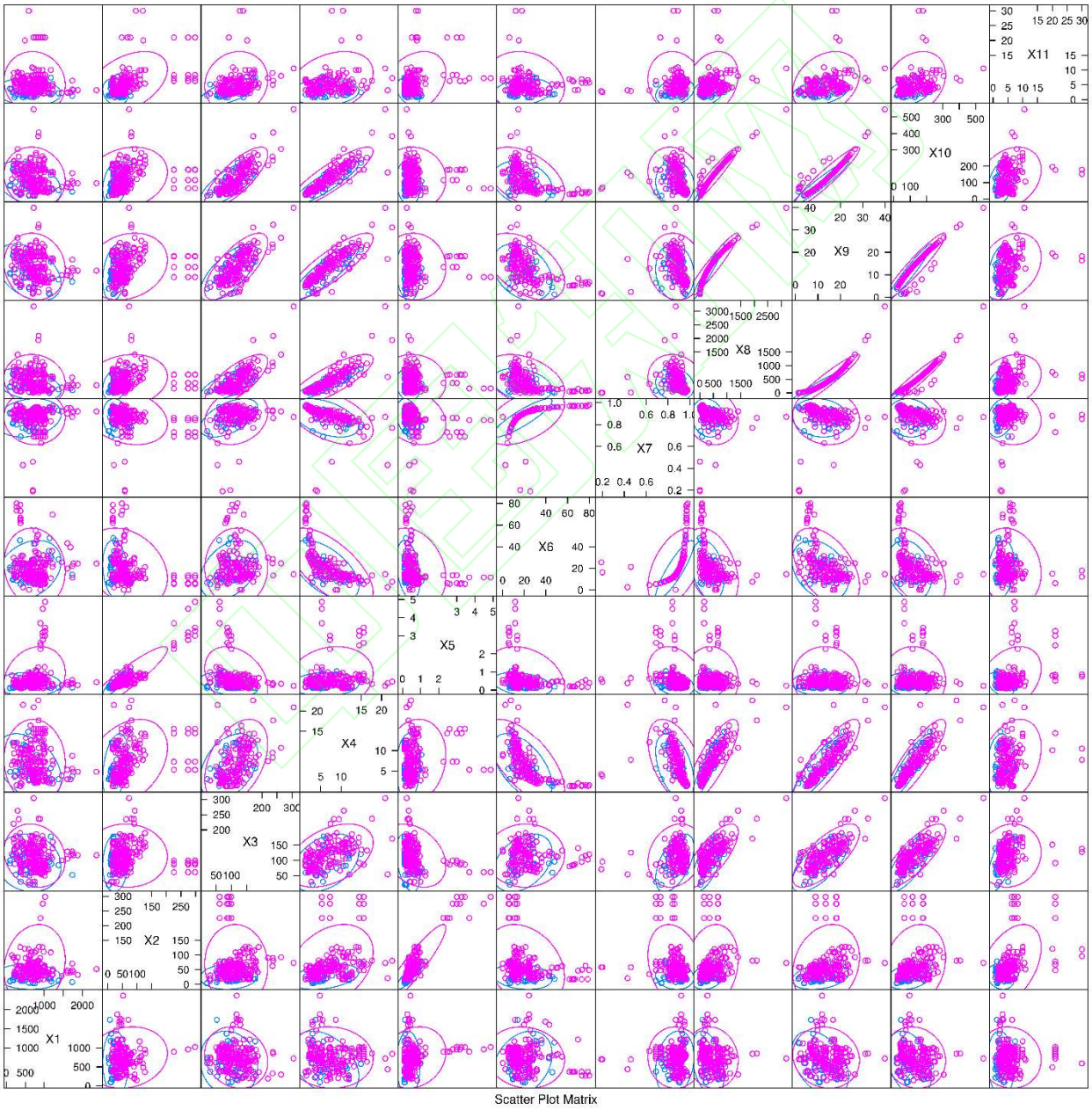

Fig. 8 Scatter plot matrix of the processed dataset

Based on the scatter plot matrix in Fig. 8, we can observe the randomness, distribution, and correlation between the input variables. Interestingly, the characteristics of the X_8, X_9, X_{10}, and X_{11} variables are

highly similar, and even with the same distributions, as shown in the crop of Fig. 9 below. Accordingly, we can see that the correlation between X_{10} and X_{11} is strong similar to the correlation between X_9 and X_{11}. In addition, the correlation between X_8 and X_{11} is not strongly like the X_9 and X_{10}, but it is also high similarity compared to pairs of X_{10}-X_{11} and X_9-X_{11}. Therefore, they should be removed to ensure the accuracy of the models. Finally, this study only used seven input parameters (from X_1 to X_7) to forecast and classify the rockburst hazards.

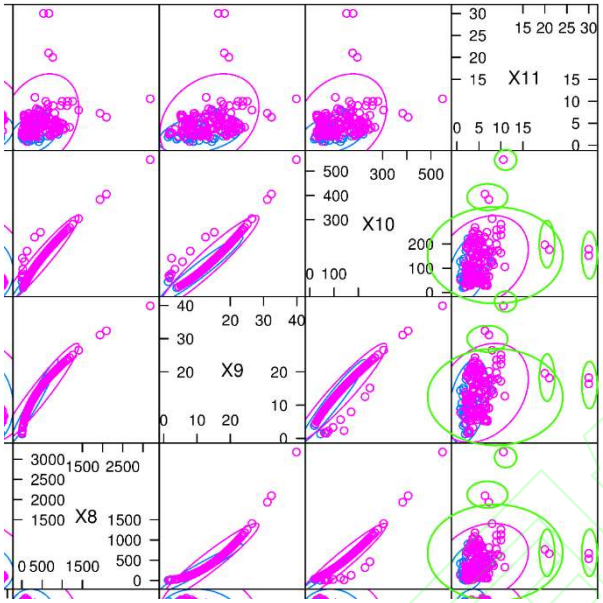

Fig. 9 A crop of scatter plot matrix and analysis of the similarities and differences between X8-X11 variables

4 Development of the models and results

To develop the GEP-PSO model for forecasting and to classify the rockburst ability, the flowchart in Fig. 4 was applied. Accordingly, an initial GEP model was developed first, and the parameters of the PSO algorithm was set up to optimize the weights of the GEP model. The initial parameters of the GEP model were set up as follow:

Number of chromosomes: 30

Head size: 8

Number of genes: from 1 to 4

Fitness function: ROC measure

Strategy: optimal evolution

Genetic operators: Mutation 0.00138; Inversion 0.00546;

Constants per gene: 10

Lower and upper bounds: [-10, 10]

Before developing the GEP-PSO models, the parameters of the PSO algorithm, including local coefficient (c_1), global coefficient (c_2), weight min factor (w_1), and weight max factor (w_2) were also setup as follows: 1.2, 1.2, 0.4, 0.9, respectively.

In GEP models, there are the initial parameters described above. The number of genes and linking functions are crucial criteria to decide on the forecast models' accuracy. Therefore, this study developed 13 different GEP models based on different genes (from 1 to 4) and linking functions (e.g., additional, subtraction, multiplication, and division). The PSO algorithm then optimized these 13 GEP models, and they are described in equations (1-13), as follow:

Model 1: This model was developed based on only one gene and without any linking functions. The PSO algorithm optimized the weights of the model, and it is described in equation (6).

$$\text{Gene 1: } \exp\left(\sqrt[4]{X_5^3 \times X_6 + \left(X_7 \times X_4\right)}\right) - X_5$$

$$\text{Rockburst} = \exp\left(\sqrt[4]{X_5^3 \times X_6 + \left(X_7 \times X_4\right)}\right) - X_5 \quad (6)$$

Model 2: This model was developed based on two genes and the addition linking function. The PSO algorithm optimized the weights of the model, and it is described in equation (7).

$$\text{Gene 1: } \log\left(X_2^3\right)$$

$$\text{Gene 2: } \tan\left(\sin\left(\left(\arctan\left(X_6\right) \times \sqrt{X_1}\right) - \left(\sqrt[4]{X_2} + X_5\right)\right)\right)$$

$$\text{Rockburst} = \log\left(X_2^3\right) + \tan\left(\sin\left(\left(\arctan\left(X_6\right) \times \sqrt{X_1}\right) - \left(\sqrt[4]{X_2} + X_5\right)\right)\right) \quad (7)$$

Model 3: This model was developed based on two genes and the subtraction linking function. It is worth noting that these genes are different from the genes developed in the Model 1 and Model 2. The PSO algorithm optimized the weights of the model, and it is described in equation (8).

$$\text{Gene 1: } \left(-3.965X_5\right)^4 \times X_7^3 \times \left(\left(X_6 - 2.544\right) + \tan\left(-2.248\right)\right)$$

$$\text{Gene 2: } \frac{\left(-0.841X_3\right)^2}{-2.862X_6 \times 2.712} \times \exp\left(\arctan\left(X_4\right)\right)$$

$$\text{Rockburst} = \left[\left(-3.965X_5\right)^4 \times X_7^3 \times \left(\left(X_6 - 2.544\right) + \tan\left(-2.248\right)\right)\right] \times \left[\frac{\left(-0.841X_3\right)^2}{-2.862X_6 \times 2.712} \times \exp\left(\arctan\left(X_4\right)\right)\right] \quad (8)$$

Model 4: This model was developed based on two genes and the multiplication linking function. It is worth noting that these genes are different from the genes which were developed in the Model 1, Model 2, and Model 3. The PSO algorithm optimized the weights of the model, and it is described in equation (9).

$$\text{Gene 1: } \left(X_2 - \left(X_4 + 16.11\right)\right) - \frac{22.727}{X_4 - 10.54}$$

Gene 2: $\sqrt[3]{\sqrt[5]{\cos\left(X_6-\frac{X_2}{X_1}\right)}}$

Rockburst =

$$\left[\left(X_2-\left(X_4+16.11\right)\right)-\frac{22.727}{X_4-10.54}\right]\times\sqrt[3]{\sqrt[5]{\cos\left(X_6-\frac{X_2}{X_1}\right)}} \quad (9)$$

Model 5: This model was developed based on two genes and the division linking function. It is worth noting that these genes are different from the genes which were developed in the Model 1 – Model 4. The PSO algorithm optimized the weights of the model, and it is described in equation (10).

Gene 1: $\frac{1}{\sqrt[3]{\sqrt[5]{\frac{1}{X_2}}}}\times\exp\left(\sqrt[5]{X_2}\right)$

Gene 2: $\frac{\sin\left(-4.558X_2\right)}{0.198}$

$$\text{Rockburst} = \frac{\frac{1}{\sqrt[3]{\sqrt[5]{\frac{1}{X_2}}}}\times\exp\left(\sqrt[5]{X_2}\right)}{\frac{\sin\left(-4.558X_2\right)}{0.198}} \quad (10)$$

Model 6: This model was developed based on three genes and the addition linking function. It is worth noting that these genes are different from the genes developed in the Model 1 – Model 5. The PSO algorithm optimized the weights of the model, and it is described in equation (11).

Gene 1: $X_5-\left[\cos\left(\tan\left(X_6\right)\right)\times\left(\sqrt[5]{X_7}-\sqrt[4]{X_5}\right)\right]$

Gene 2: $\log\left(X_3\right)$

Gene 3: $\ln\left(\sqrt[5]{\left(X_3+\left(X_7+1.698\right)\right)+\sqrt[3]{\left(-6.643-X_2\right)}}\right)$

Rockburst =

$$X_5-\left[\cos\left(\tan\left(X_6\right)\right)\times\left(\sqrt[5]{X_7}-\sqrt[4]{X_5}\right)\right]+\log\left(X_3\right)+\ln\left(\sqrt[5]{\left(X_3+\left(X_7+1.698\right)\right)+\sqrt[3]{\left(-6.643-X_2\right)}}\right) \quad (11)$$

Model 7: This model was developed based on three genes and the subtraction linking function. It is worth noting that these genes are different from the genes which were developed in the Model 1 – Model 6. The PSO algorithm optimized the weights of the model, and it is described in equation (12).

Gene 1: $\frac{X_2}{\left(\arctan\left(\left(\arctan\left(\left(\log\left(X_3\right)\right)^2\right)\right)^3\right)\right)^3}$

Gene 2: $\tan\left(X_4\right)$

Gene 3: $\sqrt[5]{X_1+\left(\tan\left(\sqrt[3]{X_3}\right)+\left(X_2-5.565\right)\right)^4}$

Rockburst =

$$\frac{X_2}{\left(\arctan\left(\left(\arctan\left(\left(\log\left(X_3\right)\right)^2\right)\right)^3\right)\right)^3}-\tan\left(X_4\right)-\sqrt[5]{X_1+\left(\tan\left(\sqrt[3]{X_3}\right)+\left(X_2-5.565\right)\right)^4} \quad (12)$$

Model 8: This model was developed based on three genes and the multiplication linking function. It is worth noting that these genes are different from the genes which were developed in the Model 1 – Model 7. The PSO algorithm optimized the weights of the model, and it is described in equation (13).

Gene 1: X_5

Gene 2: $\cos\left(\arctan\left(\left(X_2-619.415\right)^3\times\left(\left(X_1+1.149\right)\times\left(X_6+619.415\right)\right)\right)\right)$

Gene 3: $X_2+\left[\cos\left(\tan\left(X_4\right)\right)\times\left(2X_6+\left(8.19-X_4\right)\right)\right]$

Rockburst =

$$X_5\times\cos\left(\arctan\left(\left(X_2-619.415\right)^3\times\left(\left(X_1+1.149\right)\times\left(X_6+619.415\right)\right)\right)\right)\times X_2+\left[\cos\left(\tan\left(X_4\right)\right)\times\left(2X_6+\left(8.19-X_4\right)\right)\right] \quad (13)$$

Model 9: This model was developed based on three genes and the division linking function. It is worth noting that these genes are different from the genes which were developed in the Model 1 – Model 8. The PSO algorithm optimized the weights of the model, and it is described in equation (14).

Gene 1: $\left(\log\left(\frac{\sin\left(X_6\right)}{X_1+8.757}\right)^2\right)^2-X_4$

Gene 2: $\left(-2.68\frac{X_3}{1.65}+\left(-667.169-\left(X_5\times X_1\right)\right)\right)^3$

Gene 3: $\left(\arccos\left(\cos\left(\cos\left(\frac{X_4}{4.225}\right)^4\right)\right)\right)^4$

Rockburst =

$$\frac{\left(\log\left(\frac{\sin\left(X_6\right)}{X_1+8.757}\right)^2\right)^2-X_4}{\left(-2.68\frac{X_3}{1.65}+\left(-667.169-\left(X_5\times X_1\right)\right)\right)^3\times\left(\arccos\left(\cos\left(\cos\left(\frac{X_4}{4.225}\right)^4\right)\right)\right)^4} \quad (14)$$

Model 10: This model was developed based on four genes and the addition linking function. It is worth noting that these genes are different from the

genes which were developed in the Model 1 – Model 9. The PSO algorithm optimized the weights of the model, and it is described in equation (15).

Gene 1: $\sqrt{X_7}$

Gene 2: X_5^4

Gene 3: $\ln\left(\ln\left(X_1\right)\right)$

Gene 4: $1.506X_7 \times \sqrt[4]{\exp\left(\sqrt[3]{X_4}\right)}$

Rockburst =

$$X_5^4 + \ln\left(\ln\left(X_1\right)\right) + 1.506X_7 \times \sqrt[4]{\exp\left(\sqrt[3]{X_4}\right)} \quad (15)$$

Model 11: This model was developed based on four genes and the subtraction linking function. It is worth noting that these genes are different from the genes which were developed in the Model 1 – Model 10. The PSO algorithm optimized the weights of the model, described in equation (16).

Gene 1: $\left(X_3 + X_2 + X_6\right) \times \left(\exp\left(\frac{1}{X_5}\right)\right)$

Gene 2: X_5

Gene 3: $\left[8.569 - \left(\left(\left(\sqrt[5]{6.143X_5}\right)^3\right) \times X_2\right)\right]^3$

Gene 4: $\left(X_6 - 552.579\right) \times \left(X_6 - \left(X_1 + X_2\right)\right)$

Rockburst =

$$\left[\left(X_3 + X_2 + X_6\right) \times \left(\exp\left(\frac{1}{X_5}\right)\right)\right] - X_5 - \left[\left(X_6 - 552.579\right) \times \left(X_6 - \left(X_1 + X_2\right)\right)\right] \quad (16)$$

Model 12: This model was developed based on four genes and the multiplication linking function. It is worth noting that these genes are different from the genes which were developed in the Model 1 – Model 11. The PSO algorithm optimized the weights of the model, described in equation (17).

Gene 1: $\left(\left(\sqrt{X_5} - X_4\right) \times \arctan\left(X_1 + 0.297\right)\right)^2$

Gene 2: $\left(\tan\left(X_4^3\right)\right)^3 + \left(X_2 - X_5\right) + \sin\left(X_4\right)$

Gene 3: X_6

Gene 4: $\left[\cos\left(-12.269\left(\left(X_7 + X_4\right) \times X_5\right)\right) - X_5\right]^2$

Rockburst =

$$\left(\left(\sqrt{X_5} - X_4\right) \times \arctan\left(X_1 + 0.297\right)\right)^2 \times \left(\tan\left(X_4^3\right)\right)^3 + \left(X_2 - X_5\right) + \sin\left(X_4\right) \times X_6 \times \left[\cos\left(-12.269\left(\left(X_7 + X_4\right) \times X_5\right)\right) - X_5\right]^2 \quad (17)$$

Model 13: This model was developed based on four genes and the division linking function. It is worth noting that these genes are different from the genes which were developed in the Model 1 – Model 12. The PSO algorithm optimized the weights of the model, and it is described in equation (18).

Gene 1: $\tan\left(\left(\sin\left(\tan\left(\cos\left(X_5\right)\right)\right)\right)^3\right)$

Gene 2: $\frac{1}{\tan\left(\frac{X_3}{X_2} + 6.482\right)} - 2X_3$

Gene 3: $X_4 - \sin\left(\ln\left(X_7\right)\right)$

Gene 4: X_7^6

Rockburst =

$$\frac{\tan\left(\left(\sin\left(\tan\left(\cos\left(X_5\right)\right)\right)\right)^3\right)}{\left(\frac{1}{\tan\left(\frac{X_3}{X_2} + 6.482\right)} - 2X_3\right) \times \left(X_4 - \sin\left(\ln\left(X_7\right)\right)\right) \times X_7^6} \quad (18)$$

Once the GEP-PSO equations were well-established for forecasting rockburst, their performance was computed and evaluated through various metrics, such as accuracy, positive predictive value (PPV), recall, correl, F1 measure, and area under the ROC Curve (AUC). Nevertheless, it is challenging to conclude which model is the best in forecasting rockburst ability based on various metrics. Therefore, a ranking method was applied to classify and rank the models' performance. The details of the performances are shown in Tables 1 and 2.

Table 1 Performances of the GEP-PSO models with different number of genes and linking functions (training phase)

Model	Parameters		Performances						Rank for performances						
	Number of genes	Linking function	Accuracy	PPV	Recall	Correl	F1 Measure	AUC ROC	Rank for Accuracy	Rank for PPV	Rank for Recall	Rank for Correl	Rank for F1 Measure	Rank for AUC ROC	Total rank
MODEL 1	1	None	87.80	60.00	85.71	0.377	0.706	0.930	7	7	11	8	10	12	55
MODEL 2	2	Addition	85.98	58.06	64.29	0.485	0.610	0.853	4	5	3	4	1	3	20
MODEL 3	2	Subtraction	86.59	56.52	92.86	0.352	0.703	0.938	5	4	13	9	9	13	53
MODEL 4	2	Multiplication	85.37	55.00	78.57	0.47	0.647	0.900	2	3	6	5	2	7	25
MODEL 5	2	Division	87.20	59.46	78.57	0.039	0.677	0.854	6	6	6	12	7	4	41
MODEL 6	3	Addition	89.02	65.63	75.00	0.633	0.700	0.894	8	10	4	2	8	5	37
MODEL 7	3	Subtraction	90.85	72.41	75.00	0.635	0.737	0.920	11	11	4	1	12	11	50
MODEL 8	**3**	**Multiplication**	**89.63**	**64.86**	**85.71**	**0.450**	**0.738**	**0.902**	**10**	**9**	**11**	**6**	**13**	**9**	**58**
MODEL 9	3	Division	90.85	88.24	53.57	0.033	0.667	0.763	11	12	2	13	6	1	45
MODEL 10	4	Addition	89.02	64.71	78.57	0.398	0.710	0.911	8	8	6	7	11	10	50
MODEL 11	4	Subtraction	85.37	54.76	82.14	0.487	0.657	0.898	2	2	9	3	5	6	27
MODEL 12	4	Multiplication	90.85	93.33	50.00	0.066	0.651	0.785	11	13	1	10	4	2	41
MODEL 13	4	Division	84.76	53.49	82.14	0.051	0.648	0.900	1	1	9	11	3	7	32

Note: The best GEP-PSO model is shown in bold type.

Table 2 Performances of the GEP-PSO models with different number of genes and linking functions (testing phase)

Model	Parameters		Performances						Rank for performances						
	Number of genes	Linking function	Accuracy	PPV	Recall	Correl	F1 Measure	AUC ROC	Rank for Accuracy	Rank for PPV	Rank for Recall	Rank for Correl	Rank for F1 Measure	Rank for AUC ROC	Total rank
MODEL 1	1	None	74.39	40.74	68.75	0.308	0.512	0.770	5	6	8	4	8	8	39
MODEL 2	2	Addition	65.85	26.92	43.75	0.277	0.333	0.701	1	1	4	6	3	4	19
MODEL 3	2	Subtraction	70.73	36.67	68.75	0.169	0.478	0.727	3	4	8	10	7	5	37
MODEL 4	2	Multiplication	69.51	28.57	37.50	-0.065	0.324	0.519	2	2	3	13	2	1	23
MODEL 5	2	Division	74.39	36.84	43.75	0.287	0.400	0.780	5	5	4	5	5	10	34
MODEL 6	3	Addition	80.49	50.00	68.75	0.456	0.579	0.811	9	9	8	1	13	12	52
MODEL 7	3	Subtraction	80.49	50.00	62.50	0.362	0.556	0.779	9	9	6	2	12	9	47
MODEL 8	**3**	**Multiplication**	**80.49**	**50.00**	**68.75**	**0.255**	**0.529**	**0.807**	**9**	**9**	**8**	**7**	**10**	**11**	**54**
MODEL 9	3	Division	81.71	57.14	25.00	0.068	0.348	0.619	12	12	2	12	4	2	44
MODEL 10	4	Addition	78.05	45.83	68.75	0.236	0.550	0.762	7	7	8	8	11	7	48
MODEL 11	4	Subtraction	70.73	35.71	62.50	0.232	0.455	0.758	3	3	6	9	6	6	33
MODEL 12	4	Multiplication	82.93	75.00	18.75	0.090	0.300	0.679	13	13	1	11	1	3	42
MODEL 13	4	Division	79.27	47.83	68.75	0.323	0.514	0.838	8	8	8	3	9	13	49

Note: The best GEP-PSO model is shown in bold type.

5 Discussion

The PSO algorithm was applied to optimize 13 GEP models for classifying the rockburst susceptibility in deep openings. The experimental results in Tables 1 and 2 proved the high effectiveness of the proposed GEP-PSO models. Of those, the GEP-PSO models with multiple genes tend to better than the GEP-PSO model with only one gene. Nevertheless, not all models with multiple genes outperform the model with only one gene. The GEP-PSO 1 model with only one gene provided an unstable performance on the training and testing phase. Thus, it can be seen that the GEP-PSO model with only one gene and without linking function is unstable for classifying rockburst.

Considering the GEP-PSO models with multiple genes and different linking functions, it can be seen that the GEP-PSO 8 model with three genes and the multiplication linking function was used, provided the best performance on both the training and testing phases (i.e., Accuracy = 89.63, PPV = 64.86, Recall = 85.71, Correl = 0.450, F1 measure = 0.738, and AUC ROC = 0.902, and the total ranking of 58 on the training dataset; Accuracy = 80.49, PPV = 50.00, Recall = 68.75, Correl = 0.255, F1 measure = 0.529, AUC ROC = 0.807, and the total ranking of 54 on the testing dataset). Although the GEP-PSO models' performances are different; however, their accuracy is high and strongly improved with the support of the PSO algorithm, compared with that of other models in the previous studies [30, 55]. Fig. 10 shows the ROC Curve performance of the GEP-PSO models developed in this study to classify rockburst in different underground projects.

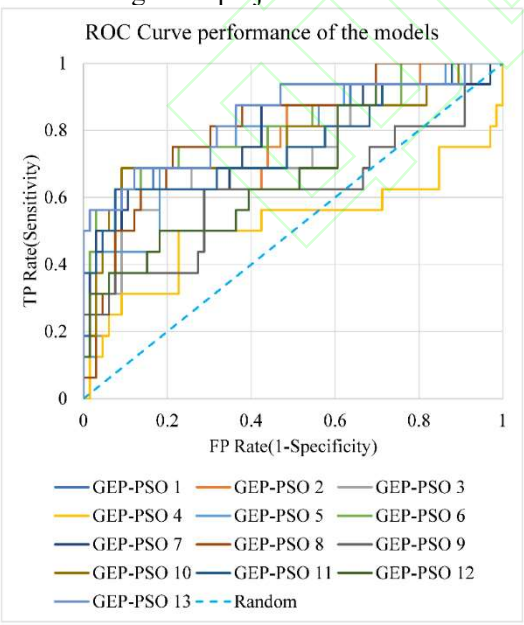

Fig. 10 ROC curve of the GEP-PSO models for classifying rockburst

It can be observed that the GEP-PSO 4 model with two genes and the multiplication linking function provided the poorest ROC Curve performance even though it used more than one gene and linking function. This finding indicates that the GEP-PSO model with two genes and the multiplication linking function should not be used for classifying rockburst in this study since its poor and unstable performance. The other GEP-PSO models are also potential models, and their implementation is acceptable.

For further assessment of the proposed hybrid PSO-based GEP models for classifying rockburst, the classification scatter plots of 13 proposed models were draw on the testing dataset based on the false negative (FN), false positive (FP), true negative (TN), true positive (TP), and the cutoff points of the models, as shown in Fig. 11. Accordingly, the best model provided the FN, FP, TN, and TP on or nearest the cutoff points. In other words, the best convergence of FN, FP, TN, TP and the cutoff points, the best model for classifying rockburst.

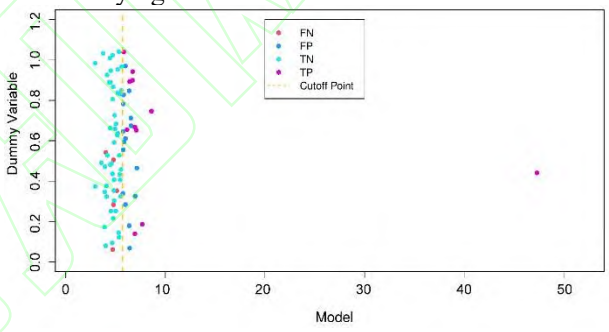

(a) Model 1

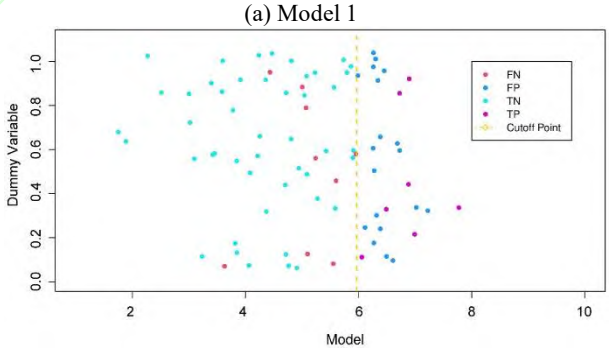

(b) Model 2

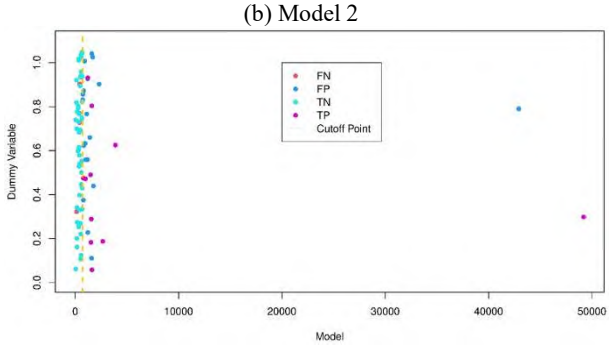

(c) Model 3

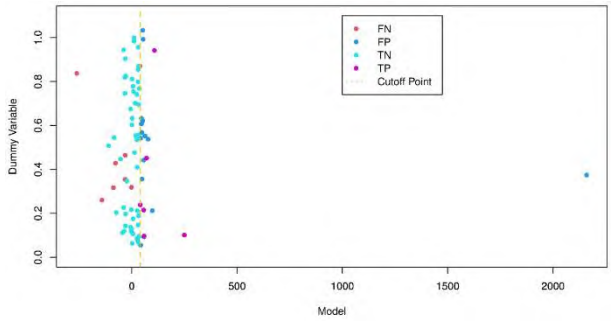

(d) Model 4

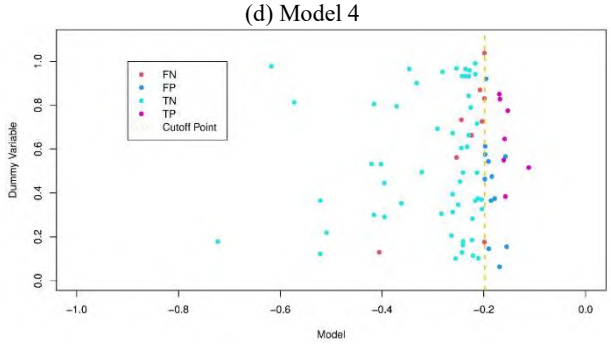

(e) Model 5

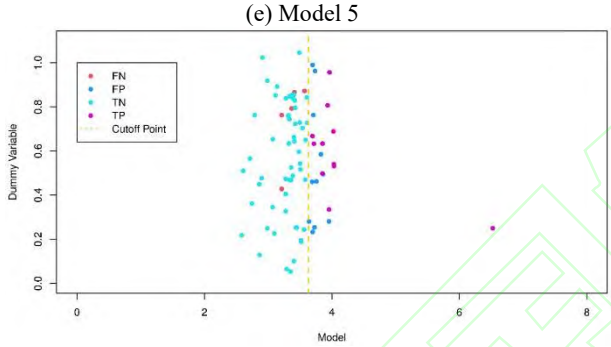

(f) Model 6

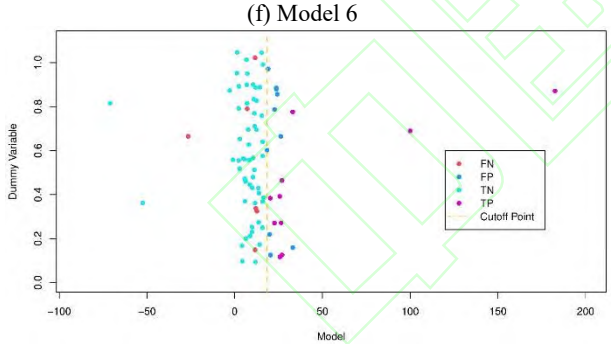

(g) Model 7

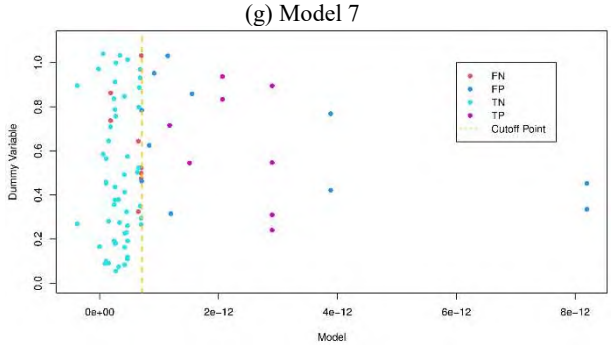

(h) Model 8

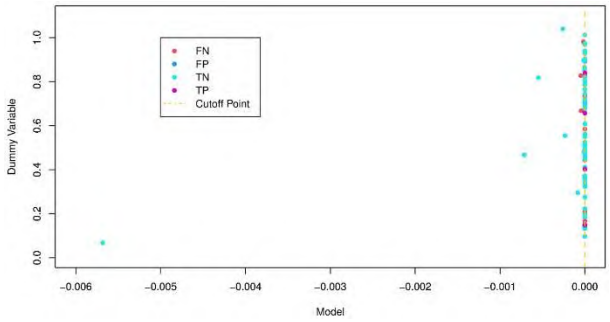

(i) Model 9

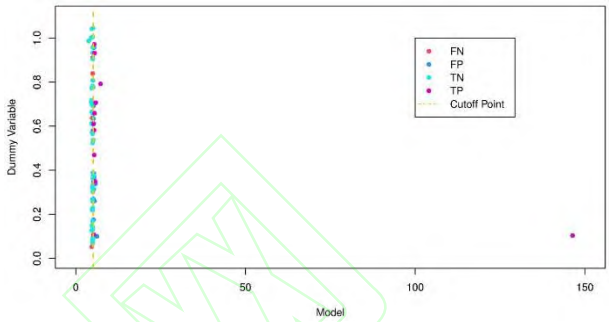

(j) Model 10

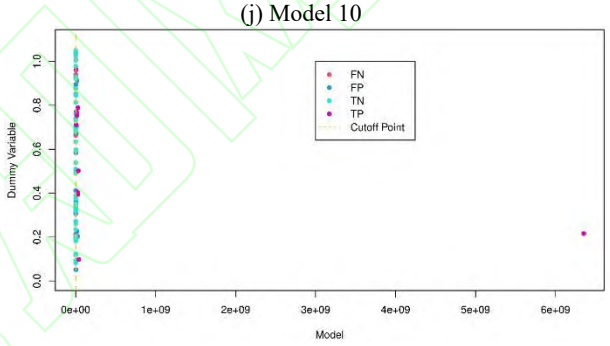

(k) Model 11

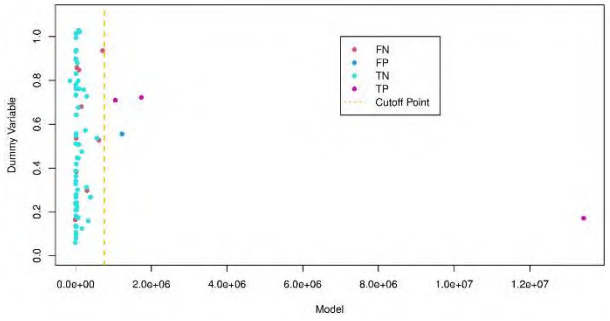

(l) Model 12

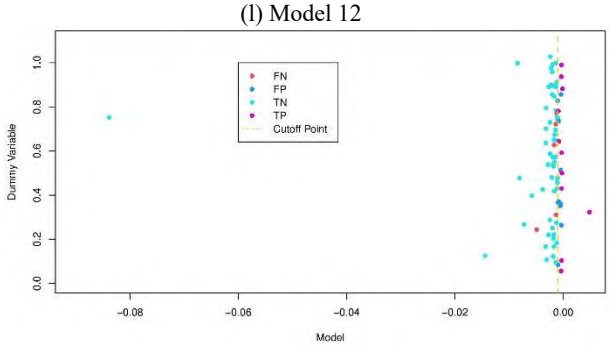

(m) Model 13

Fig. 11 Classification scatter plot of the proposed hybrid models

From the classification scatter plot of the proposed hybrid models in Fig. 11, it is clear that the

proposed hybrid GEP-PSO models provided the classification systems with pretty good accuracy. The Model 8 and Model 9 provided the highest accuracy in classifying rockburst phenomenon with greater TN and TP points. Taking a closer look at Figures 11h and 11i, it can be seen that the Model 8 model provided better accuracy than those of the Model 9 model with greater TN and TP points. The model's accuracy based on the dummy variable is very high, with the lowest range of the model and the cutoff point is approximate 0. These findings indicated that the Model 8 is the best expert system for classifying rockburst phenomenon in underground openings. A comparison of the obtained results of this study with that of the previous studies based on the same dataset is shown in Table 3.

Table 3 Comparison of the proposed GEP-PSO model (of this work) and previous models (by previous researchers)

References	Model	Inputs	Accuracy
[30]	GBM	X_1, X_2, X_3, X_4, X_5, X_6, X_{11}	76.6%
[59]	Cloud model with rough set	X_1, X_2, X_3, X_4, X_5, X_6, X_{11}	71.05%
This study	GEP-PSO	X_1, X_2, X_3, X_4, X_5, X_6, X_7	80.49%

Based on the comparisons of Table 3, we can see that this study also used seven input parameters; however, the last input variable is different from the previous studies. X7 variable was used instead of X11 in the previous studies based on the data analyses of the collected database. This finding indicated that the X7 variable should be used instead of the X11 variable to get better performance with the proposed GEP-PSO model.

6 Validation of the models

To demonstrate the selected hybrid GEP-PSO model's accuracy, we used six other observations as the unseen dataset in practice. It is worth noting that these observations have not been used to develop the models and tested on the testing dataset. The input parameters of these six observations were entered into the selected hybrid model to validate the outcome predictions. Finally, they were compared with the experimental results to decide the developed expert systems. The input parameters of the validation dataset and the forecasted results are shown in Table 4.

Table 4. Validation dataset and the forecasted results of the proposed GEP-PSO model

X_1	X_2	X_3	X_4	X_5	X_6	X_7	Y	GEP-PSO	Match
500	25.34	90	6.55	0.52	16.25	0.83	0	0	OK (TN)
535	47.06	125	7.5	0.36	22.15	0.9	0	0	OK (TN)
458	34.66	85.96	8.12	0.65	18.22	0.85	1	0	Wrong (FN)
605	21.08	80.5	5.44	0.28	25.35	0.95	0	0	OK (TN)
780	68.25	92.35	7.12	0.88	14.25	0.88	1	1	OK (TP)
850	77.62	115.2	8.55	0.76	28.19	0.9	1	1	OK (TP)

Based on the forecasted results in Table 4, it can be seen that the classification accuracy and error of the selected GEP-PSO model is pretty high, with an accuracy of 83.33% (i.e., 5 correct predictions and 1 wrong prediction). The predicted results on the validation dataset are summarized in Table 5 through the classification accuracy and error, and confusion matrix. These results demonstrated that the proposed and selected GEP-PSO model is a potential expert system to predict the practice's rockburst phenomenon. It is a useful tool to prevent the rockburst tendency.

Table 5. Summary of the predicted results on the validation dataset

Validation data summary:		
Classification Accuracy & Error		
	Counts	Percent
Correct:	5	83.33%
Wrong:	1	16.67%

Confusion matrix		
	Yes (predicted)	No (predicted)
Yes (actual)	2	1
No (actual)	0	3

Confusion matrix (in percentages)		
	Yes (predicted)	No (predicted)
Yes (actual)	33.33%	16.67%
No (actual)	0.00%	50.00%

7 Conclusions and remarks

Rockburst hazard is a geological phenomenon encountered in deep openings and tunnels that lead to injuries and deaths, damaged equipment, and deformation of underground/tunnel faces. Due to those adverse effects, soft computational models for predicting and classifying rockburst grades are considered potential approaches to early warning the rockburst susceptibility and evaluating the intensity

of rockburst. This study proposed a novel soft computational model, i.e., the GEP-PSO model, to predict and classify rockburst tendency with high accuracy. The results showed that the accuracy of the proposed GEP-PSO model was significantly improved based on the corrected values of missing values and the number of genes and linking functions of the GEP model. Besides, the PSO algorithm also played an essential role in improving the accuracy of the GEP model. The obtained results indicated that the proposed GEP-PSO model provided a superior accuracy compared with that of the published classification models. In conclusion, the GEP-PSO model should be used as an expert system in practical engineering to warn the rockburst susceptibility and prevent this phenomenon from reducing this severe problem's losses.

Acknowledgments

The authors would like to thank the Centre for Mining, Electro-Mechanical Research, Hanoi University of Mining and Geology (HUMG), Hanoi, Vietnam for their kind supports.

Conflicts of Interest

The authors declare no conflict of interest.

References

[1] LI T, CAI M F, CAI M. A review of mining-induced seismicity in China [J]. International Journal of Rock Mechanics and Mining Sciences, 2007, 44(8): 1149-1171.

[2] LIANG W Z, ZHAO G Y, WANG X, et al. Assessing the rockburst risk for deep shafts via distance-based multi-criteria decision making approaches with hesitant fuzzy information [J]. Engineering Geology, 2019, 260: 105211.

[3] TURCHANINOV I, MARKOV G. Conditions of changing of extra-hard rock into weak rock under the influence of tectonic stresses of massifs [C]//ISRM International Symposium 1981, International Society for Rock Mechanics and Rock Engineering, 1981.

[4] LI T B, MA C C, ZHU M L, et al. Geomechanical types and mechanical analyses of rockbursts [J]. Engineering Geology, 2017, 222: 72-83.

[5] MA C C, LI T B, ZHANG H, et al. A method for numerical simulation based on microseismic information and the interpretation of hard rock fracture [J]. Journal of Applied Geophysics, 2019, 164: 214-224.

[6] WANG Y Q, CHANG H T, WANG J Y, et al. Countermeasures to treat collapse during the construction of road tunnel in fault zone: a case study from the Yezhuping Tunnel in south Qinling, China [J]. Environmental Earth Sciences, 2019, 78(15): 1-16.

[7] LI Z Q, XUE Y G, LI S C, et al. Rock burst risk assessment in deep-buried underground Caverns: A novel analysis method [J]. Arabian Journal of Geosciences, 2020, 13(11): 1-11.

[8] MAŁKOWSKI P, NIEDBALSKI Z. A comprehensive geomechanical method for the assessment of rockburst hazards in underground mining [J]. International Journal of Mining Science and Technology, 2020, 30(3): 345-355.

[9] IANNACCHIONE A T, ZELANKO J C. Occurrence and remediation of coal mine bumps: a historical review [C]// Proceedings of the Mechanics and Mitigation of Violent Failure in Coal and Hard-Rock Mines, 1995: 27-67.

[10] POTVIN Y, HUDYMA M, JEWELL R J. Rockburst and seismic activity in underground Australian mines: An introduction to a new research project [C]//ISRM international symposium 2000, International Society for Rock Mechanics and Rock Engineering, 2000.

[11] BLAKE W, HEDLEY D G. Rockbursts: Case studies from North American hard-rock mines [M]. Englewood: Society for Mining Metallurgy & Exploration, 2004.

[12] SHI Q, PAN Y S, LI Y J. The typical cases and analysis of rockburst in China [J]. Coal Mining Technology, 2005, 10(2): 13-17.

[13] WONDRAD M, CHEN D. Application of mine seismicity monitoring technology in mitigating geotechnical risks at Barrick's Darlot Gold Mine [C]//Golden Rocks 2006, The 41st US Symposium on Rock Mechanics (USRMS), 2006. American Rock Mechanics Association, 2006

[14] BALTZ R, HUCKE A. Rockburst prevention in the German coal industry [C]//Proceedings of the 27th International Conference on Ground Control in Mining, West Virginia University, Morgantown, WV, 2008: 46-50.

[15] DOU L M, CAI W, GONG S Y, et al. Dynamic risk assessment of rock burst based on the technology of seismic computed tomography detection [J]. Journal of China Coal Society, 2014, 39(2): 238-244.

[16] LI Z L, DOU L M, WANG G F, et al. Risk evaluation of rock burst through theory of static and dynamic stresses superposition [J]. Journal of Central South University, 2015, 22(2): 676-683.

[17] PHAM N A, OSINSKI P, DO N A, et al. Numerical modeling of slope stability incorporating complex reinforcement solution in high-risk failure area- unusual case study [J]. Journal of Mining and Earth Sciences, 2021, 62(6): 48-57.

[18] GOH A T C, ZHANG Y M, ZHANG R H, et al. Evaluating stability of underground entry-type excavations using multivariate adaptive regression splines and logistic regression [J]. Tunnelling and Underground Space Technology, 2017, 70: 148-154.

[19] NGUYEN T T, INDRARATNA B, CARTER J. Laboratory investigation into biodegradation of jute drains with implications for field behavior [J]. Journal of Geotechnical and Geoenvironmental Engineering, 2018, 144(6): 04018026.

[20] ZHANG W G, LI H R, WU C Z, et al. Soft computing approach for prediction of surface settlement induced by earth pressure balance shield tunneling [J]. Underground Space, 2021, 6(4): 353-363.

[21] ZHANG W G, ZHANG R H, WU C Z, et al. State-of-the-art review of soft computing applications in underground

excavations [J]. Geoscience Frontiers, 2020, 11(4): 1095-1106.

[22] LE D T, BUI T M. Numerical modelling techniques for studying longwall geotechnical problems under realistic geological structures [J]. Journal of Mining and Earth Sciences, 2021, 62(3): 87-96.

[23] LONG N Q. Accuracy assessment of open - pit mine's digital surface models generated using photos captured by Unmanned Aerial Vehicles in the post - processing kinematic mode [J]. Journal of Mining and Earth Sciences, 2021, 62(4), 38-47.

[24] NGUYEN H M, LE A N, NGUYEN M D, et al. Application of seismic attribute analysis in Lower Miocene reservoir characterization, northeast Bach Ho field, Vietnam [J]. Journal of Mining and Earth Sciences, 2021, 62(6): 14-22.

[25] RAHAL F, HAMED F Z B, HADJEL M. Mapping of clay soils exposed to the shrinking-swelling phenomenon, with EO-1-Hyperion data in the region of Sidi-Chahmi, Algeria [J]. Journal of Mining and Earth Sciences, 2021, 62(6): 1-7.

[26] VU D H, NGUYEN H T. Estimation of shale volume from well logging data using Artificial Neural Network [J]. Journal of Mining and Earth Sciences, 2021, 62(3): 46-52.

[27] DONG L J, LI X B, PENG K. Prediction of rockburst classification using Random Forest [J]. Transactions of Nonferrous Metals Society of China, 2013, 23(2): 472-477.

[28] WANG C L, WU A X, LU H, et al. Predicting rockburst tendency based on fuzzy matter-element model [J]. International Journal of Rock Mechanics and Mining Sciences, 2015, 75: 224-232.

[29] CAI M F. Prediction and prevention of rockburst in metal mines - A case study of Sanshandao gold mine [J]. Journal of Rock Mechanics and Geotechnical Engineering, 2016, 8(2): 204-211.

[30] ZHOU J, LI X B, MITRI H S. Classification of rockburst in underground projects: comparison of ten supervised learning methods [J]. Journal of Computing in Civil Engineering, 2016, 30(5): 04016003.

[31] PU Y Y, APEL D B, LINGGA B. Rockburst prediction in kimberlite using decision tree with incomplete data [J]. Journal of Sustainable Mining, 2018, 17(3): 158-165.

[32] PU Y Y, APEL D B, XU H W. Rockburst prediction in kimberlite with unsupervised learning method and support vector classifier [J]. Tunnelling and Underground Space Technology, 2019, 90: 12-18.

[33] ZHOU J, KOOPIALIPOOR M, LI E M, et al. Prediction of rockburst risk in underground projects developing a neuro-bee intelligent system [J]. Bulletin of Engineering Geology and the Environment, 2020, 79(8): 4265-4279.

[34] XUE Y G, BAI C H, QIU D H, et al. Predicting rockburst with database using particle swarm optimization and extreme learning machine [J]. Tunnelling and Underground Space Technology, 2020, 98: 103287.

[35] SHIRANI FARADONBEH R, SHAFFIEE HAGHSHENAS S, TAHERI A, et al. Application of self-organizing map and fuzzy c-mean techniques for rockburst clustering in deep underground projects [J]. Neural Computing and Applications, 2020, 32(12): 8545-8559.

[36] ZHANG J F, WANG Y H, SUN Y T, et al. Strength of ensemble learning in multiclass classification of rockburst intensity [J]. International Journal for Numerical and Analytical Methods in Geomechanics, 2020, 44(13): 1833-1853.

[37] HE S Y, LAI J X, ZHONG Y J, et al. Damage behaviors, prediction methods and prevention methods of rockburst in 13 deep traffic tunnels in China [J]. Engineering Failure Analysis, 2021, 121: 105178.

[38] ZHOU J, GUO H Q, KOOPIALIPOOR M, et al. Investigating the effective parameters on the risk levels of rockburst phenomena by developing a hybrid heuristic algorithm [J]. Engineering with Computers, 2021, 37(3): 1679-1694.

[39] FERREIRA C. (2006). Gene expression programming: Mathematical modeling by an artificial intelligence [M]. Verlag Berlin Heidelberg: Springer, 2006.

[40] SARIDEMIR M. Genetic programming approach for prediction of compressive strength of concretes containing rice husk ash [J]. Construction and Building Materials, 2010, 24(10): 1911-1919.

[41] KABOLI S H A, FALLAHPOUR A, SELVARAJ J, et al. Long-term electrical energy consumption formulating and forecasting via optimized gene expression programming [J]. Energy, 2017, 126: 144-164.

[42] HAJIHASSANI M, JAHED ARMAGHANI D, MONJEZI M, et al. Blast-induced air and ground vibration prediction: a particle swarm optimization-based artificial neural network approach [J]. Environmental Earth Sciences, 2015, 74(4): 2799-2817.

[43] BUI X N, JAROONPATTANAPONG P, NGUYEN H, et al. A novel hybrid model for predicting blast-induced ground vibration based on k-nearest neighbors and particle swarm optimization [J]. Scientific Reports, 2019, 9: 13971.

[44] ZHANG X L, NGUYEN H, BUI X N, et al. Novel soft computing model for predicting blast-induced ground vibration in open-pit mines based on particle swarm optimization and XGBoost [J]. Natural Resources Research, 2020, 29(2): 711-721.

[45] NGUYEN H, BUI H B, BUI X N. Rapid determination of gross calorific value of coal using artificial neural network and particle swarm optimization [J]. Natural Resources Research, 2021, 30(1): 621-638.

[46] ZHANG X L, NGUYEN H, BUI X N, et al. Evaluating and predicting the stability of roadways in tunnelling and underground space using artificial neural network-based particle swarm optimization [J]. Tunnelling and Underground Space Technology, 2020, 103: 103517.

[47] KENNEDY J, EBERHART R. Particle swarm optimization [C]//Proceedings of ICNN'95 - International Conference on Neural Networks. November 27 - December 1, 1995, Perth, WA, Australia. IEEE, 1995: 1942-1948.

[48] SHI Y, EBERHART R C. Parameter selection in particle swarm optimization [C]//International Conference on Evolutionary Programming, 1998: 591-600.

[49] EBERHART, SHI Y H. Particle swarm optimization: developments, applications and resources [C]//Proceedings of the 2001 Congress on Evolutionary Computation (IEEE Cat. No.01TH8546). May 27-30, 2001, Seoul, Korea (South). IEEE, 2001: 81-86.

[50] POLI R, KENNEDY J, BLACKWELL T. Particle swarm optimization [J]. Swarm Intelligence, 2007, 1(1): 33-57.

[51] KENNEDY J. Particle swarm optimization [M]//Encyclopedia of machine learning, Springer, 2011: 760-766.

[52] SHANTHI M, MEENAKSHI D K, RAMESH P K. Particle swarm optimization [M]// PARSOPOULOS K E, VRAHATIS M N. Advances in swarm intelligence for optimizing problems in computer science, Chapman and Hall/CRC, 2018: 115-144.

[53] SLOWIK A. Particle swarm optimization [M]//Intelligent systems, 2018.

[54] WANG D S, TAN D P, LIU L. Particle swarm optimization algorithm: An overview [J]. Soft Computing, 2018, 22(2): 387-408.

[55] ZHOU J, LI X B, SHI X Z. Long-term prediction model of rockburst in underground openings using heuristic algorithms and support vector machines [J]. Safety Science, 2012, 50(4): 629-644.

[56] ADOKO A C, GOKCEOGLU C, WU L, et al. Knowledge-based and data-driven fuzzy modeling for rockburst prediction [J]. International Journal of Rock Mechanics and Mining Sciences, 2013, 61: 86-95.

[57] MA T H, TANG C N, TANG S B, et al. Rockburst mechanism and prediction based on microseismic monitoring [J]. International Journal of Rock Mechanics and Mining Sciences, 2018, 110: 177-188.

[58] JUNNINEN H, NISKA H, TUPPURAINEN K, et al. Methods for imputation of missing values in air quality data sets [J]. Atmospheric Environment, 2004, 38(18): 2895-2907.

[59] LIN Y, ZHOU K P, LI J L. Application of cloud model in rock burst prediction and performance comparison with three machine learning algorithms [J]. IEEE Access, 2018, 6: 30958-30968.